Data in Brief 31 (2020) 105791

Contents lists available at ScienceDirect

Data in Brief

journal homepage: www.elsevier.com/locate/dib

Data Article

Mineralogical dataset of natural zeolites from Lessini Mounts, Northern Italy: Analcime, natrolite, phillipsite and harmotome chemical composition

Michele Mattioli*, Marco Cenni

Department of Pure and Applied Sciences, University of Urbino Carlo Bo, Italy

ARTICLE INFO

Article history:
Received 9 May 2020
Revised 21 May 2020
Accepted 25 May 2020
Available online 2 June 2020

Keywords:
Zeolites
Secondary minerals
Basalts
Lessini Mounts
Veneto Volcanic Province

ABSTRACT

This dataset article contains mineralogical and chemical data of some natural zeolites such as analcime, natrolite, phillipsite and harmotome. These minerals were found as secondary phases within vesicles and veins in the basaltic rocks of the Lessini Mounts, Northern Italy. Methods for obtaining the datasets include optical microscopy, X-ray diffraction, scanning electron microscopy and electron probe microanalysis. Analcime forms well-developed, transparent to milky crystals with a typical icositetrahedron habit. The average composition of analcime is calculated as $Na_{13.79}Ca_{0.01}K_{0.03}Ba_{0.03}[Al_{14.28}Si_{33.82}O_{96}]$ $16H_2O$, with all of the extra-framework sites occupied by sodium. Natrolite usually forms hemispherical aggregates with glassy, colourless to white thin prismatic crystals, which generally radiate from a central point. The average chemical composition of natrolite is $Na_{14.28}Ca_{0.14}K_{0.01}[Al_{15.60}Si_{24.59}O_{80}]$ $16H_2O$. Crystals of phillipsite-harmotome serie occur in a variety of forms and display a highly variable chemical composition, from almost pure compositions to intermediate values. Phillipsite is more common and its average chemical composition is $Ca_{1.40}Na_{0.29}K_{1.08}Ba_{0.27}[Al_{4.68}Si_{11.28}O_{32}]$ $12H_2O$, while harmotome is rare and has an average chemical composition of $Ca_{0.97}Na_{0.20}K_{0.36}Ba_{0.91}[Al_{4.60}Si_{11.46}O_{32}]$ $12H_2O$. The obtained dataset can be used for various purposes: it can be used by

* Corresponding author.
E-mail address: michele.mattioli@uniurb.it (M. Mattioli).

https://doi.org/10.1016/j.dib.2020.105791

other authors to compare morphological features and chemical compositions of similar zeolites crystals discovered in other parts of the world, it can be compared with those obtained from similar geologic environments encouraging studies on hydrothermal processes, and it could represent the starting point for a potential exploration of zeolites from an industrial point of view.

Specifications Table

Subject	Earth and Planetary Sciences
Specific subject area	Geology, mineralogy, zeolites
Type of data	Tables, images, graphics
How data were acquired	Optical microscope: stereo binocular Zeiss KL1500 LCD. Powder X-ray powder diffraction (XRD): Philips X'Change PW1830 powder diffractometer. Scanning Electron Microscopes (SEM): Philips 515 equipped with EDAX 9900, and Jeol 6400 with an Oxford Link Isis. Electron Micro Probe (EMP): four wavelength dispersion spectrometers Cameca Camebax Microbeam 799.
Data format	Raw, analyzed
Parameters for data collection	• About 300 samples of mineralized cavities were collected in the field, forty-four of which were selected and analysed. • Each cavity was studied using a binocular microscope. • Pure crystals were separated from each sample, disaggregated and carefully pulverized in an agate mortar for detailed, long exposures (up to 24 h) XRD analysis; analytical conditions were 35 kV accelerating potential, 30 mA filament current, Bragg–Brentano geometry, 2–70° 2 θ, step size 0.01° 2 θ and 2.5 s counting time/step. • Representative fragments of mineralized cavities and isolated crystals were mounted in aluminum stub for SEM observations and analysis; operating conditions were a 15 kV accelerating potential and a 2 to 15 nA beam current. • Selected crystals were incorporated in epoxy resin in order to obtain polished thin sections for EMP analysis; analyzes performed with an electronic beam diameter of about 5–7 µm, an acceleration potential of 15 kV and a beam current of 10 nA. • The electron beam was defocused, with a shortened accumulation time (from 100 s down to 50 s) to minimizes volatile migration and loss. The standards used were natural minerals and synthetic phases. The analyses were selected on the basis of their low chemical balance (E%): zeolites with an E% $>$ 10 were rejected.
Description of data collection	• The secondary minerals were identified from their physical properties and extracted from cavities using a binocular microscope. • Powder X-ray diffraction (XRD) was used to confirm and identify the selected crystals, to evaluate their quality and to exclude the presence of impurities. • Scanning Electron Microscopy (SEM) and Energy Dispersion Spectroscopy (EDS) was used to define their morphology and verify the semi-quantitative elemental composition. • Chemical composition of selected minerals was finally determined using wavelength dispersive spectroscopy on an EMP.

(*continued on next page*)

Data source location	Alpone Valley, Lessini Mounts, Veneto Region, Northern Italy 45° 31′ 0″ N, 11° 14′ 0″ E
Data accessibility	With the article
Related Research Article	M. Mattioli, M. Cenni, E. Passaglia, Secondary mineral assemblages as indicators of multistage alteration processes in basaltic lava flows: Evidence from the Lessini Mountains, Veneto Volcanic Province, Northern Italy, Periodico di Mineralogia 85 (2016) 1–24 [1].

Value of the Data

- Analcime, natrolite, phillipsite and harmotome zeolite crystals from Lessini Mounts, Northern Italy, have been detected and chemically characterized for both local and global comparisons.
- These zeolites could potentially be exploitable from an industrial point of view for their peculiar physical properties.
- The data presented here may be used by other authors to compare morphological features and chemical compositions of other similar zeolite crystals discovered in other parts of the world.
- The data can be compared with those obtained from similar geologic environments and motivate studies on hydrothermal mineralizations in the future.

1. Data description

This data article contains mineralogical and chemical data of some natural zeolites from the Lessini Mounts in Veneto Region, Northern Italy (Fig. 1) [1]. This area has recently been the subject of interest for the discovery of potentially toxic fibrous zeolites, such as erionite [2–4]. In this dataset further natural zeolites which crystallize in association with erionite, e.g., analcime, natrolite, phillipsite and harmotome, were identified and characterized by optical microscopy, X-ray diffraction, scanning electron microscopy and electron probe microanalysis. Morphology and other physical properties of the investigated zeolites are shown in Figs. 2 and 3, while their chemical composition obtained from electron probe microanalysis is reported in Tables 1–4, and illustrated in Fig. 4.

Analcime forms well-developed, transparent to milky crystals up to 5 mm in diameter with a typical icositetrahedron {211} habit (Fig. 2a). It is generally colourless, but white, gray, pink, pale yellow, greenish and reddish crystals can also be found. It can occur either as individual crystals or as clusters in veins and cavities. The average composition of analcime is $Na_{13.79}Ca_{0.01}K_{0.03}Ba_{0.03}[Al_{14.28}Si_{33.82}O_{96}]\ 16H_2O$ and has a homogeneous chemical composition, with all of the extra-framework sites occupied by sodium (Table 1). The Si/(Si+Al) ratio varies from 0.70 to 0.71, which are slightly higher values than those observed in the literature for analcime from amygdales in basalts (~0.67) [5]. The Na/(Na+Ca) ratio is always ~1, as are the mono- and bivalent cation ratios. Analcime from vesicles and cavities has no differences in composition to that analyzed from fractures and veins.

Natrolite can usually be found as hemispherical aggregates, up to 5 mm in diameter, with glassy, colourless to white thin prismatic crystals, which commonly radiate from a central point (Fig. 2b). The crystals (up to 2 mm) are dominated by a prism with a well-formed tetragonal section, truncated by pyramids. Many of the prism faces have a very thin coating of clay minerals as botryoidal aggregates. The average chemical composition of natrolite is $Na_{14.28}Ca_{0.14}K_{0.01}[Al_{15.60}Si_{24.59}O_{80}]\ 16H_2O$ (Table 2), which is very close to the stoichiometric formula [5]. The Si/(Si+Al) ratio varies from 0.59 to 0.62, while sodium is in the range 13.61 – 14.98 apfu and calcium is always < 1 apfu.

Phillipsite-harmotomes occur in a variety of forms (Fig. 3). They can typically be found as lustrous, glassy, short prismatic crystals of 0.5–2 mm in size, often forming dense, interpenetrating crystal aggregates. In places, these crystals are parallel-aligned contact twins consisting of three individual fourling twins. Phillipsite-harmotome can also occur as linings of densely matted tiny crystals that completely line vesicles and vugs, or as spherules and botryoidal radial aggregates (up to 5 mm) of closely matted, glassy, prismatic crystals that completely coat vesicle

Table 1
Representative EMP chemical compositions of analcime from the Lessini Mounts. E% (balance error) = [(Al-Al_{theor})/Al_{theor}] × 100, where Al_{theor} = (Na+K) + 2(Ca+Mg+Sr+Ba), according to [9]; *R* = Si/(Si+Al); M/(M+B) = (Na+K)/(Na+K+Ca+Mg+Sr+Ba); - = analysed but below detection limit.

	ANA1	ANA2	ANA3	ANA4	ANA5	ANA6	ANA7	ANA8	ANA9	ANA10	ANA11	ANA12
SiO2	59.12	58.69	59.29	58.55	58.94	58.51	58.77	57.94	58.52	58.75	59.12	58.88
Al2O3	20.91	20.97	21.31	20.96	21.28	20.86	20.78	21.18	21.23	20.72	21.23	20.74
Fe2O3	–	–	–	–	–	0.1	0.05	0.05	0.04	–	–	
MgO	–	–	–	–	0.03	0.01	0.06	–	–	0.02	–	0.01
MnO	–	–	–	–	–	–	–	–	–	–	–	
BaO	0.3	0.37	–	0.15	0.26	0.18	–	–	–	–	–	0.25
SrO	–	–	–	–	–	–	–	–	–	–	–	
CaO	0.02	–	0.01	–	0.01	–	0.09	0.04	–	–	–	0.01
Na2O	12.23	12.45	12.59	12.74	12.38	12.41	12.27	11.89	12.03	12.48	12.55	12.26
K2O	0.05	0.04	0.04	0.01	0.01	–	0.07	0.01	0.08	0.05	0.06	0.02
H2O	7.37	7.49	6.76	7.58	7.09	7.92	7.9	8.89	8.1	7.98	7.04	7.83
Total	100	100	100	100	100	100	100	100	100	100	100	100
apfu based on 96 oxygens												
Si	33.94	33.81	33.79	33.75	33.75	33.82	33.9	33.72	33.78	33.88	33.74	33.91
Al	14.15	14.24	14.31	14.24	14.36	14.21	14.13	14.53	14.45	14.21	14.35	14.23
Fe	–	–	–	–	–	–	–	–	–	–	–	–
Mg	–	–	–	–	0.03	0.01	0.52	–	–	0.01	–	0.01
Ba	0.07	0.08	–	0.03	0.06	0.04	–	–	–	–	–	0.08
Sr	–	–	–	–	–	–	–	–	–	–	–	–
Ca	0.01	–	0.01	–	0.01	–	0.06	0.03	–	–	–	0.01
Na	13.61	13.9	13.91	14.24	13.75	13.91	13.72	13.42	13.46	13.95	13.88	13.72
K	0.04	0.03	0.03	0.01	0.01	–	0.05	0.01	0.06	0.02	0.02	0.05
E%	2.47	0.97	2.6	−0.5	3.1	1.75	1.16	8.00	6.95	1.77	2.85	4.15
R	0.71	0.7	0.7	0.7	0.7	0.7	0.71	0.7	0.7	0.7	0.7	0.7
M/(M+B)	0.99	0.99	1.00	1.00	0.99	1.00	0.96	1.00	1.00	1.00	1.00	0.99

Table 2
Representative EMP chemical compositions of natrolite from the Lessini Mounts. E% (balance error) = [(Al-Al_{theor})/Al_{theor}] × 100, where Al_{theor} = (Na+K) + 2(Ca+Mg+Sr+Ba), according to [9]; R = Si/(Si+Al); M/(M+B) = (Na+K)/(Na+K+Ca+Mg+Sr+Ba); - = analysed but below detection limit.

	NAT1	NAT2	NAT3	NAT4	NAT5	NAT6	NAT7	NAT8	NAT9	NAT10	NAT11	NAT12
SiO2	49.45	49.21	50.46	47.7	48.71	48.51	49.00	49.95	49.22	47.98	49.11	49.15
Al2O3	25.92	25.98	25.82	26.02	25.95	28.27	28.11	25.88	25.94	26.01	27.13	26.05
Fe2O3	0.01	–	–	0.01	0.01	–	–	–	–	0.01	–	–
MgO	–	–	–	0.01	–	–	–	–	–	–	–	–
BaO	0.29	0.07	0.22	0.07	–	0.22	0.29	0.11	0.25	0.15	–	0.05
SrO	–	–	–	–	–	–	–	–	–	–	–	–
CaO	0.17	0.1	0.01	0.85	0.05	0.74	0.15	0.12	0.05	0.23	0.1	0.64
Na2O	13.99	15.33	14.06	14.19	14.85	14.36	15.22	14.55	14.74	14.22	15.44	14.88
K2O	–	0.04	–	–	–	0.01	–	–	0.03	–	–	–
H2O	10.17	9.27	9.43	11.14	10.43	7.89	7.23	9.39	9.77	11.4	8.22	9.23
Total	100	100	100	100	100	100	100	100	100	100	100	100
apfu based on 80 oxygens												
Si	24.95	24.71	25.19	24.46	24.71	23.99	24.09	24.98	24.68	24.55	24.14	24.66
Al	15.42	15.38	15.19	15.72	15.51	16.48	16.29	15.44	15.31	15.26	15.24	16.01
Fe	–	–	–	–	–	–	–	–	–	–	–	–
Mg	–	–	–	0.01	–	–	–	–	–	–	–	–
Ba	0.06	0.01	0.04	0.01	–	0.04	0.06	0.02	0.05	0.03	–	0.01
Sr	–	–	–	–	–	–	–	–	–	–	–	–
Ca	0.09	0.05	0.01	0.47	0.03	0.39	0.08	0.06	0.03	0.07	0.05	0.31
Na	13.69	14.92	13.61	14.1	14.6	13.77	14.51	14.2	14.45	13.98	14.98	14.52
K	–	0.03	–	–	–	0.01	–	–	0.02	–	–	–
E%	10.26	1.13	10.86	4.28	5.87	12.53	10.24	5.54	6.65	4.55	8.97	1.33
R	0.62	0.62	0.62	0.61	0.61	0.59	0.6	0.62	0.62	0.62	0.61	0.61
$M/(M+B)$	0.99	1.00	1.00	0.97	1.00	0.97	0.99	0.99	0.99	0.99	1.00	0.98

Table 3
Representative EMP chemical compositions of phillipsite from the Lessini Mounts. E% (balance error) = [(Al-Al$_{theor}$)/Al$_{theor}$] × 100, where Al$_{theor}$ = (Na+K) + 2(Ca+Mg+Sr+Ba), according to [9]; R = Si/(Si+Al); M/(M+B) = (Na+K)/(Na+K+Ca+Mg+Sr+Ba); - = analysed but below detection limit.

	PHI1	PHI2	PHI3	PHI4	PHI5	PHI6	PHI7	PHI8	PHI9	PHI10	PHI11	PHI12	PHI13	PHI14	PHI15	PHI16	PHI17	PHI18	PHI19	PHI20	PHI21	PHI22	PHI23	PHI24
SiO2	50.7	56.28	55.11	54.57	55.53	54.83	54.13	54.49	54.38	54.95	55.34	53.88	52.07	54.61	57.22	52.28	50.18	54.38	50.76	46.76	54.12	53.32	46.15	58.12
Al2O3	20.65	16.98	18.77	19.16	18.55	18.27	19.11	19.00	18.62	18.7	18.85	18.69	20.01	17.85	18.89	20.24	18.36	18.34	18.21	17.56	20.33	20.19	20.7	17.55
Fe2O3	0.04	–	0.02	–	–	–	–	0.06	–	–	0.05	0.01	0.06	0.11	–	0.04	–	0.36	0.02	0.07	0.2	0.1	0.05	–
MgO	0.01	0.01	0.02	–	0.04	0.03	–	–	–	–	–	0.05	–	–	0.83	–	0.15	0.01	0.16	0.04	–	0.08	0.03	0.05
BaO	5.29	8.87	4.46	4.57	4.43	3.74	4.75	4.96	5.64	4.32	4.35	6.4	3.63	9.98	0.07	0.3	0.44	0.93	0.11	0.37	0.22	0.19	0.35	0.11
SrO	–	–	–	–	–	0.09	–	–	–	–	–	0.12	–	–	0.71	–	–	–	–	–	–	–	–	–
CaO	7.22	3.58	5.95	6.14	6.00	6.04	6.18	5.94	5.96	6.09	6.18	5.91	7.01	4.12	8.05	6.58	5.03	7.05	4.93	6.29	6.89	7.1	6.55	8.13
Na2O	0.49	0.65	0.72	0.9	0.91	0.58	0.41	0.64	1.04	0.6	0.85	0.12	0.54	1.06	0.65	0.53	1.6	0.37	1.33	0.97	0.24	0.41	1.15	0.45
K2O	3.12	3.21	3.13	3.17	2.93	2.86	2.39	3.1	3.71	3.32	3.41	2.87	3.35	3.02	1.5	6.7	5.9	4.00	7.42	5.1	5.59	7.31	7.86	3.12
H2O	12.47	10.41	11.82	11.49	11.62	13.57	13.03	11.79	10.65	12.03	10.97	11.94	13.32	9.25	12.07	13.33	18.34	14.55	17.05	22.84	12.4	11.3	17.06	12.47
Total	100	100	100	100	100	100	100	100	100	100	100	100	100	100	100	100	100	100	100	100	100	100	100	100
apfu based on 32 oxygens																								
Si	10.8	11.81	11.43	11.34	11.48	11.52	11.36	11.36	11.33	11.43	11.4	11.36	11.02	11.49	11.47	10.98	11.16	11.42	11.18	11.02	11.13	10.99	10.74	11.54
Al	5.19	4.2	4.59	4.69	4.52	4.52	4.73	4.67	4.57	4.59	4.58	4.65	4.99	4.43	4.46	5.01	4.81	4.54	4.73	4.88	4.93	4.9	4.75	4.42
Fe	0.01	–	–	–	–	–	–	0.01	–	–	0.01	–	0.01	0.02	–	0.01	–	0.06	–	0.01	0.03	0.02	0.01	–
Mg	–	–	0.01	–	–	0.01	–	–	–	–	–	0.02	–	–	0.25	–	0.05	–	0.05	0.01	–	0.03	0.01	0.25
Ba	0.44	0.73	0.36	0.37	0.36	0.31	0.39	0.41	0.46	0.35	0.35	0.53	0.3	0.82	0.01	0.03	0.04	0.08	0.01	0.03	0.02	0.02	0.03	0.01
Sr	–	–	–	–	–	0.01	–	–	–	–	–	0.02	–	–	0.08	–	–	–	–	–	–	–	–	–
Ca	1.65	0.81	1.32	1.37	1.33	1.36	1.39	1.33	1.33	1.36	1.36	1.34	1.59	0.93	1.73	1.48	1.2	1.59	1.16	1.59	1.52	1.57	1.58	1.68
Na	0.2	0.26	0.29	0.24	0.37	0.24	0.17	0.26	0.42	0.24	0.34	0.05	0.22	0.43	0.25	0.22	0.69	0.15	0.57	0.44	0.1	0.16	0.45	0.24
K	0.85	0.86	0.83	0.84	0.77	0.77	0.64	0.82	0.99	0.88	0.9	0.77	0.91	0.81	0.38	1.8	1.67	1.07	2.09	1.53	1.47	1.92	1.66	0.58
E%	−0.84	0.04	2.06	2.91	−0.38	3.34	8.25	2.89	−8.32	0.96	−1.73	0.81	1.92	−6.35	−6.35	−0.09	−2.51	0.74	−7.3	−6.84	7.02	−7.18	1.18	4.55
K/(K+Ba)	0.66	0.54	0.7	0.69	0.68	0.71	0.62	0.67	0.68	0.72	0.72	0.59	0.75	0.5	0.97	0.98	0.98	0.93	1	0.98	0.99	0.99	0.98	0.98
R	0.68	0.74	0.71	0.71	0.72	0.72	0.71	0.71	0.71	0.71	0.71	0.71	0.69	0.72	0.72	0.69	0.7	0.72	0.7	0.69	0.69	0.69	0.69	0.72
M/(M+B)	0.33	0.42	0.4	0.38	0.4	0.37	0.31	0.38	0.44	0.4	0.42	0.3	0.37	0.41	0.23	0.57	0.65	0.42	0.69	0.55	0.5	0.56	0.57	0.3

Table 4
Representative EMP chemical compositions of harmotome from the Lessini Mounts. E% (balance error) = $[(\text{Al-Al}_{\text{theor}})/\text{Al}_{\text{theor}}] \times 100$, where $\text{Al}_{\text{theor}} = (\text{Na+K}) + 2(\text{Ca+Mg+Sr+Ba})$, according to [9]; R = Si/(Si+Al); M/(M+B) = (Na+K)/(Na+K+Ca+Mg+Sr+Ba); - = analysed but below detection limit.

	HAR1	HAR2	HAR3	HAR4	HAR5	HAR6	HAR7	HAR8	HAR9	HAR10	HAR11	HAR12	HAR13	HAR14	HAR15	HAR16	HAR17	HAR18	HAR19	HAR20	HAR21	HAR22	HAR23	HAR24
SiO2	50.41	56.94	56.12	54.56	53.53	52.29	53.69	52.67	53.77	54.13	53.51	53.08	54.38	49.62	53.24	54.07	53.68	54.39	53.8	53.06	53.89	52.85	49.55	56.98
Al2O3	16.62	17.49	17.74	19.00	18.21	17.72	19.03	18.88	18.17	18.89	18.87	19.08	18.17	17.31	19.24	18.68	18.36	18.29	18.25	17.6	18.3	19.04	17.82	17.56
Fe2O3	–	0.11	–	–	–	0.03	–	0.07	0.01	–	0.02	–	0.07	–	0.11	0.01	–	–	–	0.02	0.01	0.09	–	–
MgO	0.02	0.04	–	–	–	–	0.01	–	–	–	0.1	–	–	0.01	0.03	0.05	0.04	–	0.03	0.09	0.02	–	0.01	–
BaO	20.4	11.79	10.09	8.31	10.32	8.93	8.03	9.31	10.08	9.46	8.05	8.09	9.41	19.38	6.97	10.37	9.96	9.19	10.65	12.43	10.78	4.97	19.87	10.84
SrO	–	–	0.03	–	–	0.15	–	0.21	–	0.06	0.12	0.12	–	0.18	–	–	–	–	–	0.12	–	–	0.15	–
CaO	0.37	4.11	3.62	5.94	4.11	4.6	5.54	5.2	4.28	5.15	4.94	5.24	4.81	0.58	6.04	4.7	4.89	4.94	4.54	3.06	4.24	6.58	0.55	4.25
Na2O	0.21	0.07	0.5	0.78	0.88	1.00	0.53	0.33	0.69	0.5	0.62	0.31	0.55	0.15	0.15	0.84	0.19	0.72	0.13	0.44	1.19	0.29	0.12	0.05
K2O	0.14	1.76	2.64	1.33	1.74	1.95	1.44	1.04	1.63	1.33	1.36	1.29	1.39	0.13	1.82	1.56	0.93	1.4	1.06	1.07	1.84	1.42	0.11	1.23
H2O	11.83	7.69	9.26	10.08	11.22	13.33	11.74	12.3	11.38	10.48	12.4	12.79	11.23	12.65	12.41	9.72	11.94	11.08	11.54	12.11	9.72	14.77	11.82	9.09
Total	100	100	100	100	100	100	100	100	100	100	100	100	100	100	100	100	100	100	100	100	100	100	100	100
apfu based on 32 oxygens																								
Si	11.61	11.74	11.69	11.34	11.45	11.41	11.34	11.3	11.48	11.38	11.38	11.34	11.51	11.47	11.27	11.37	11.5	11.48	11.5	11.57	11.4	11.3	11.42	11.78
Al	4.51	4.25	4.36	4.66	4.59	4.56	4.74	4.78	4.57	4.68	4.73	4.8	4.53	4.62	4.8	4.63	4.62	4.55	4.6	4.53	4.56	4.8	4.68	4.26
Fe	–	–	–	–	–	0.01	–	0.01	–	–	–	–	0.01	–	0.02	–	–	–	–	–	–	0.01	–	–
Mg	0.01	0.01	–	–	–	–	0.03	–	–	–	0.03	–	–	–	0.01	0.02	0.01	–	0.01	0.03	0.01	–	–	–
Ba	1.84	0.95	0.82	0.68	0.87	0.76	0.66	0.78	0.84	0.78	0.67	0.68	0.78	1.76	0.58	0.86	0.83	0.76	0.89	1.06	0.89	0.42	1.84	0.94
Sr	–	–	–	–	–	0.02	–	0.03	–	0.01	0.02	0.02	–	0.02	–	–	–	–	–	0.02	–	–	0.02	–
Ca	0.09	0.91	0.81	1.32	0.94	1.08	1.25	1.2	0.98	1.16	1.13	1.2	1.09	0.14	1.37	1.06	1.12	1.12	1.04	0.72	0.96	1.51	0.15	0.9
Na	0.09	0.03	0.2	0.31	0.37	0.42	0.22	0.14	0.29	0.2	0.26	0.13	0.23	0.07	0.06	0.34	0.08	0.3	0.05	0.19	0.49	0.12	0.06	0.03
K	0.04	0.46	0.7	0.35	0.48	0.54	0.39	0.29	0.44	0.36	0.37	0.35	0.38	0.04	0.49	0.42	0.25	0.38	0.29	0.3	0.5	0.39	0.04	0.45
E%	12.44	0.75	4.37	−0.24	2.98	−2.54	6.52	8.04	4.58	5.11	9.82	12.71	4.63	10.15	7.84	0.28	8.44	2.82	8.83	9.72	−3.01	10.52	9.97	1.25
K/(K+Ba)	0.02	0.33	0.46	0.34	0.36	0.42	0.37	0.27	0.34	0.32	0.36	0.34	0.33	0.02	0.46	0.33	0.23	0.33	0.25	0.22	0.36	0.48	0.02	0.32
R	0.72	0.73	0.73	0.71	0.71	0.71	0.71	0.7	0.72	0.71	0.71	0.7	0.72	0.71	0.7	0.71	0.71	0.72	0.71	0.72	0.71	0.71	0.71	0.73
M/(M+B)	0.06	0.21	0.36	0.25	0.32	0.34	0.24	0.18	0.29	0.22	0.25	0.2	0.25	0.05	0.22	0.28	0.14	0.27	0.15	0.21	0.35	0.21	0.05	0.21

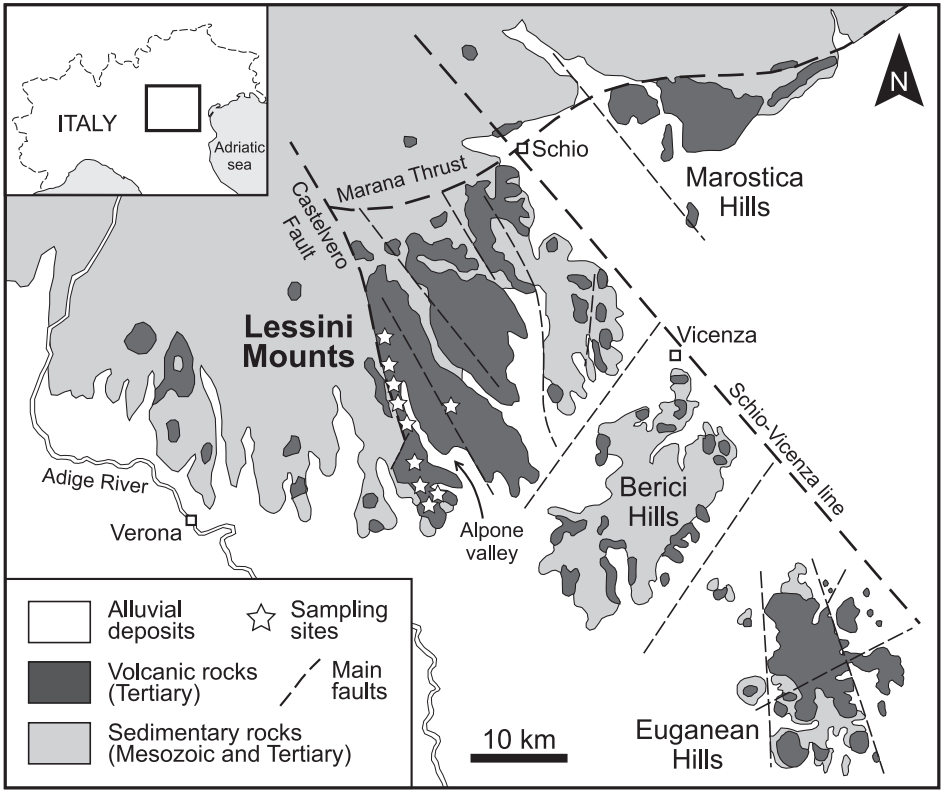

Fig. 1. Simplified geological map of the Veneto Volcanic Province showing the Lessini Mounts and location of the studied samples (modified from [1]).

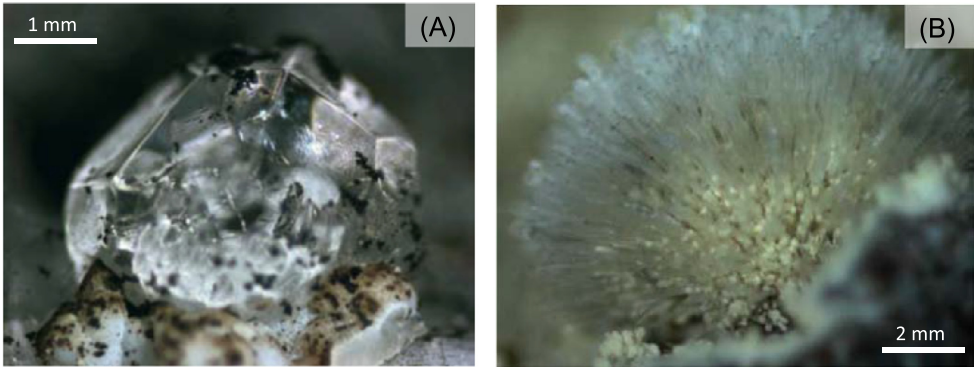

Fig. 2. Photomicrographs showing the morphology of analcime and natrolite from the Lessini Mounts (modified from [1]). (A) Well-developed, transparent crystals of analcime with the typical icositetrahedron {211} habit. (B) Sub-spherical form of glassy, colourless, thin prismatic crystals of natrolite radiating from a central point.

walls. Phillipsite is much more common than harmotome, and its average chemical composition is $Ca_{1.40}Na_{0.29}K_{1.08}Ba_{0.27}[Al_{4.68}Si_{11.28}O_{32}]\ 12H_2O$ (Table 3). The Si/(Si+Al) ratio ranges from 0.68 to 0.74, whereas the Na/(Na+Ca) and K/(*K*+Ba) ratios are in the range of 0.06–0.33 and 0.5–1 apfu, respectively. The dominant extra-framework cations are potassium and calcium, which vary from 0.38 to 2.09 and from 0.81 to 1.73, respectively (Fig. 4). Other cations are absent or very

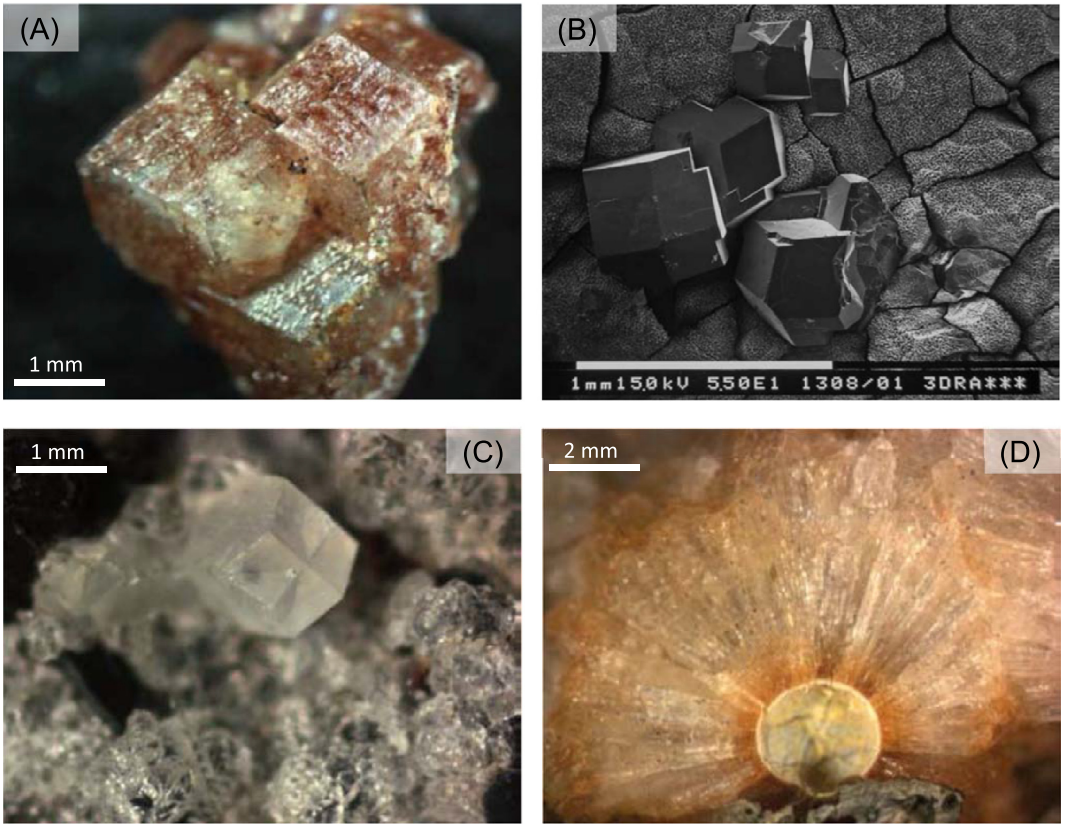

Fig. 3. Photomicrographs (A-C-D) and scanning electron microscopy images (B) showing the morphology of phillipsite-harmotome from the Lessini Mounts (modified from [1]). (A) Lustrous, whitish to reddish, short prismatic crystals of phillipsite. (B) (C) Well-shaped, transparent phillipsite crystal consisting of two sets of penetration twins. (D) Radial aggregate of closely matted, glassy, prismatic crystals forming a sub-spherical shape.

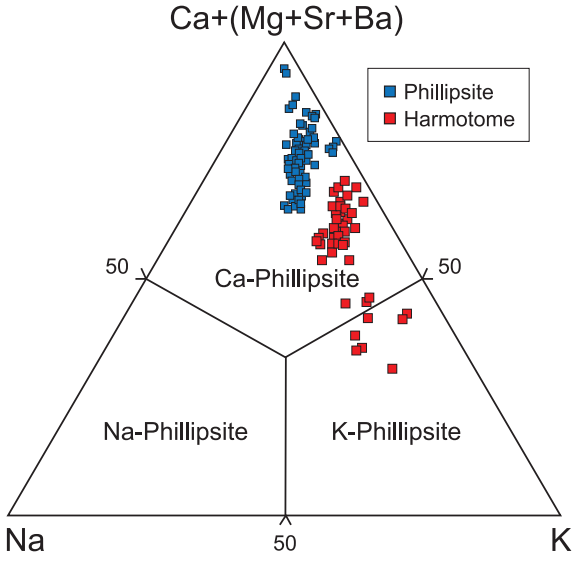

Fig. 4. (Ca+Mg+Sr+Ba)-Na-K composition plot of the phillipsite-harmotome from the Lessini basalts, showing the distribution of extra-framework cations.

low. Harmotome has an average chemical composition of $Ca_{0.97}Na_{0.20}K_{0.36}Ba_{0.91}[Al_{4.60}Si_{11.46}O_{32}]$ $12H_2O$ (Table 4), with a Si/(Si+Al) ratio ranging from 0.70 to 0.73, a K/(*K*+Ba) ratio between 0.02 and 0.48, and a Na/(Na+Ca) ratio from 0.03 to 0.50. Barium and calcium are the dominant extra-framework cations (average 0.91 and 0.97 apfu, respectively), whereas potassium is low (average 0.36 apfu) and other cations are always < 1 apfu (Fig. 4). The different chemical compositions of phillipsite and harmotome do not generally correspond to particular differences in morphology and other physical properties. However, spherules and botryoidal radial aggregates usually correspond to barium-rich compositions, whereas transparent, colourless individual crystals frequently match the phillipsite pure member

2. Experimental design, materials, and methods

2.1. Study area description

The studied samples come from several localities along the Alpone Valley, in the Lessini Mounts, Northern Italy (Fig. 1). Here, the Tertiary basalts of the Veneto Volcanic Province [6,7,8] are often deeply weathered and show a wealth of cavities and vugs filled with secondary minerals. A large number of samples (~300) were collected in the field from veins and cavities, forty-four of which were analysed in detail. The secondary phases are mainly zeolites and clay minerals, which represent ~90 vol.% of the total secondary minerals [1].

2.2. Optical microscopy

Specimens were investigated using a stereo binocular Zeiss KL1500 LCD, and images of the zeolite crystals were acquired using a digital camera AXIO CAM MRc.

2.3. X-ray diffraction (XRD)

Powder X-ray diffraction (XRD) was used to identify the studied crystals, to evaluate their quality and to exclude the presence of impurities. The XRPD patterns were recorded using a Philips X'Change PW 1830 X-ray diffractometer (Cu Kα radiation, $\lambda = 1.54056$ Å) at the University of Urbino (Italy). The samples were run between 2° and 70° 2θ. The analytical conditions were 35 kV accelerating potential and 30 mA filament current. Data were collected in Bragg–Brentano geometry from 2 to 70° 2 θ, with a step size of 0.01° 2 θ and 2.5 s counting time for each step. The following software packages were used for the measurements and subsequent analysis: X'Pert Quantify 3.0 for data collection and instrument control, and X'Pert HighScore 3.0 for semiquantitative phase analysis. All of the powder samples were prepared by side-loading an aluminum holder to obtain a quasi-random orientation.

2.4. Scanning electron microscopy (SEM)

In order to define their morphology and verify the semi-quantitative elemental composition, the studied zeolites were examined by Scanning Electron Microscopy (SEM) and Energy Dispersion Spectroscopy (EDS) using a Philips 515 equipped with EDAX 9900 at the University of Urbino (Italy), and a Jeol 6400 with an Oxford Link Isis at the University of Parma (Italy). The operating conditions were 15 kV accelerating potential and 2 to 15 nA beam current. The electron beam was defocused, which is associated with a shortened accumulation time (from 100 s down to 10 s) and minimizes volatile migration and loss. The standards used were natural minerals and synthetic phases. With these optimized experimental conditions, no significant differences between the SEM-EDS and EMPA data sets were observed, indicating the reliability of the collected data.

2.5. Electron microprobe (EMP)

Selected crystals of the examined zolites were separated under a binocular microscope, taking care to isolate only crystals free of inclusions or alterations. Subsequently, these crystals were incorporated in epoxy resin in order to obtain thin sections. After polishing and metallization, the sections were analyzed for the chemical composition with an electron microprobe equipped with four wavelength dispersion spectrometers Cameca Camebax Microbeam 799, of the CNR Center of Geosciences and Georesources, installed at the Department of Mineralogy and Petrology of the University of Padua. The analyzes were performed with an electronic beam diameter of about 5–7 µm, an acceleration potential of 15 kV and a beam current of 10 nA. Chemical data, reported in Tables 1–4, were collected from several individual point analyses for each sample, depending on the number of crystals available. In elongated crystals or crystal aggregates, several point analyses were performed along the prisms to check for chemical homogeneity. The point analyses of each sample were highly consistent, showing a variation of major elements within 2–3% of the estimated instrumental errors and indicating a high degree of chemical homogeneity within each sample. The final chemical formula is the result of the average of 12 to 24 analysis points selected on the basis of their low chemical balance (E%). The charge balance of zeolite formulas is a reliable measure for the quality of the analysis. It correlates with the extent of thermal decomposition of zeolites during microprobe analysis. A useful test is based on the charge balance between the non-framework cations and the amount of tetrahedral Al [9]. Analyses are considered acceptable if the balance error $E\% = [(Al(+Fe^{3+})\text{-}Al_{theor})/Al_{theor}] \times 100$, where $Al_{theor} = (Na+K)+2(Ca+Mg+Sr+Ba)$, is less than $\pm 10\%$ [9].

Declaration of Competing Interest

The authors declare that they have no known competing financial interests or personal relationships which have, or could be perceived to have, influenced the work reported in this article.

Acknowledgments

We thank E. Salvioli Mariani and L. Valentini for their kind help and advices with the SEM, and R. Carampin for his great expertise with the EMP. Very constructive suggestions by an anonymous reviewer and the Managing Editor significantly improved the manuscript. This work was funded in the framework of the 2018 research programs of the Department of Pure and Applied Sciences of the University of Urbino Carlo Bo (project "New asbestiform fibers: mineralogical and physical-chemical characterization", responsible M. Mattioli). Field work was supported by the Geological Mineralogical Association of Verona AGMV.

References

[1] M. Mattioli, M. Cenni, E. Passaglia, Secondary mineral assemblages as indicators of multistage alteration processes in basaltic lava flows: evidence from the Lessini Mountains, Veneto Volcanic Province, Northern Italy, Period. Mineral. 85 (2016) 1–24, doi:10.2451/2015PM0375.
[2] M. Mattioli, M. Giordani, M. Dogan, M. Cangiotti, G. Avella, R. Giorgi, A.U. Dogan, M.F. Ottaviani, Morpho-chemical characterization and surface properties of carcinogenic zeolite fibers, J. Hazard. Mater. 306 (2016) 140–148, doi:10.1016/j.jhazmat.2015.11.015.
[3] M. Giordani, M. Mattioli, P. Ballirano, A. Pacella, M. Cenni, M. Boscardin, L. Valentini, Geological occurrence, mineralogical characterization, and risk assessment of potentially carcinogenic erionite in Italy, J. Toxicol. Environ. Health Part B Crit. Rev. 20 (2017) 81–103, doi:10.1080/10937404.2016.1263586.
[4] M. Giordani, M. Mattioli, M. Dogan, A.U. Dogan, Potential carcinogenic erionite from Lessini Mounts, NE Italy: morphological, mineralogical and chemical characterization, J. Toxicol. Environ. Health Part A Curr. Issues 79 (2016) 808–824, doi:10.1080/15287394.2016.1182453.
[5] E. Passaglia, R.A. SheppardD.L. Bish, D.W. Ming (Eds.), The crystal chemistry of zeolites, Rev. Mineral. Geochem. 45 (2001) 69–116.
[6] L. Milani, L. Beccaluva, M. Coltorti, Petrogenesis and evolution of the Euganean magmatic complex, Veneto Region, North-East Italy, Eur. J. Mineral. 11 (1999) 379–399.
[7] C. Bonadiman, M. Coltorti, L. Milani, L. Salvini, F. Siena, R. Tassinari, Metasomatism in the lithospheric mantle and its relationships to magmatism in the Veneto Volcanic Province, Italy, Period. Mineral. 70 (2001) 333–357.
[8] D. Zampieri, Tertiary extension in the southern Trento Platform, Southern Alps, Italy, Tectonics 14 (1995) 645–657.
[9] E. Passaglia, The crystal chemistry of chabazites, Am. Mineral. 55 (1970) 1278–1301.